RAPID COMMUNICATION

Photoluminescence properties of porous InP filled with ferroelectric polymers

C.H. Jia · Y.H. Chen · Y.C. Jiang · F.Q. Liu · S.C. Qu · W.F. Zhang · Z.G. Wang

Abstract Photoluminescence properties of porous InP are found to be strongly affected by infilling ferroelectric polymers. Based on the temperature- and excitation-power-dependent photoluminescence, the intensity suppression and blue shift of the near-band-edge emission are supposed to result from the passivation of surface states by introducing ferroelectric polymers. On the other hand, the significant enhancement of deep-level emission is caused by the increased concentration of phosphorus vacancies due to ion exchange when infilling the ferroelectric polymers into porous InP. The surface passivation of porous InP by ferroelectric polymers is useful for improving the performances of InP-based electronic and optoelectronic devices.

1 Introduction

Recently, the formation of porous InP has been extensively studied by a simple electrochemical process for future photonic crystals, quantum electronics, optoelectronic devices, and chemical sensors [1, 2]. An attractive possibility in the photonic crystal structures is to replace the low-index part (air) with a material that has a tunable refractive index. Liquid crystals are particularly useful for such purpose

C.H. Jia · W.F. Zhang
Key Laboratory of Photovoltaic Materials of Henan Province and School of Physics & Electronics, Henan University, Kaifeng 475004, P.R. China

C.H. Jia · Y.H. Chen (✉) · Y.C. Jiang · F.Q. Liu · S.C. Qu · Z.G. Wang
Key Laboratory of Semiconductor Material Science, Institute of Semiconductors, Chinese Academy of Science, P.O. Box 912, Beijing 100083, P.R. China
e-mail: yhchen@red.semi.ac.cn
Fax: +86-10-82305052

because of the large polarization-dependent refractive index [3], but the inherent slow tuning speed and liquid state could limit the compatibility with other processing steps [4]. Hence, other materials, notably ferroelectric polyvinylidene fluoride and trifluoroethylene copolymers, P(VDF–TrFE), whose refractive index can be tuned in a large scale by an external electric field and lattice strain, are highly desirable [5, 6]. A tunable photonic crystal may be realized by infiltrating these copolymers into porous InP to form a composite. In addition, the composites also provide an interesting system to study how the ferroelectric behaviors of the polymers are influenced by the external stress, interface conditions, and finite size effect, since the ferroelectric properties are sensitive to these effects. Meanwhile, the ferroelectric polymers are quite attractive as potential dielectric, passivation, or diffusion barrier layers for InP gates because of their low cost, large-area application, and easy solution processability [7]. The ferroelectric polymers are also expected to tune the photoluminescence properties of porous InP [8]. In this paper, we fabricated the nanocomposites of porous InP infilled with ferroelectric copolymers by combining the electrochemical and high-temperature-solution infiltration processes, and studied their photoluminescence (PL) properties.
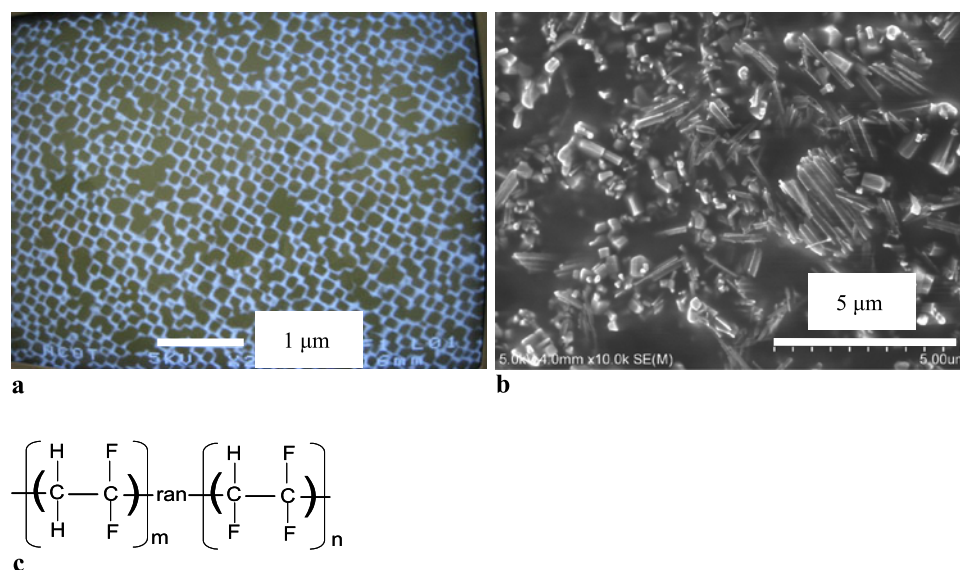
2 Experimental

The porous InP was prepared by photoanodic etching of S-doped InP (001) single crystal with a doping concentration of 4.9×10^{18} cm^{-3} (Hall) [9]. It was performed using a standard cell with three electrodes, i.e. an InP electrode, a Pt counter electrode, and a reference saturated calomel electrode. The electrolyte used was 2 M HCl (200 ml) + HNO$_3$ (6 ml) aqueous solution. The optimized overpoten-

a

b

c

tial on the InP electrode with respect to the reference saturated calomel electrode and the anodization time were 6 V and 30 s, respectively. Before preparation for infiltration, the top layer of porous substrate was etched in HBr:HNO$_3$ solution in order to unfold the pores. The copolymers of the 70 % vinylidene fluoride with 30 % trifluoroethylene, P(VDF–TrFE) 70:30, were dissolved in dimethylformamide (DMF) with a concentration of 2 wt.% by weight. In order to infiltrate the copolymers into the narrow pores, a high-temperature-solution infiltration process at 90 °C for 30 min was adopted. After the infiltration, the samples were kept at 150 °C for 10 min to let the solvent evaporate and fill the copolymers into the pores occupied by the solvent. The above procedures were repeated three times to enhance the infiltration. Finally, the sample was annealed at 150 °C for 1 h to improve the crystallization of the copolymers, and this sample was named as 'FE-treated'. For comparison, another sample was simply annealed at the same condition, named as 'heated'. For the structural characterization of porous samples, surface and cross-sectional scanning electron microscope (SEM, JSM-6301F) observations were carried out. The presence of ferroelectric polymers embedded in porous InP is confirmed by Fourier transform infrared (FTIR) transmission (Bruker, IFS120HR). PL properties for the as-grown, heated, and FE-treated samples were investigated under various temperatures and excitation powers using a Fourier-transform spectrometer equipped with a solid-state laser emitting at 532 nm and an InGaAs detector (Bruker, IFS120HR).

3 Results and discussion

Figure 1a and b show the surface SEM images of the as-grown and FE-treated porous InP films, where the dark
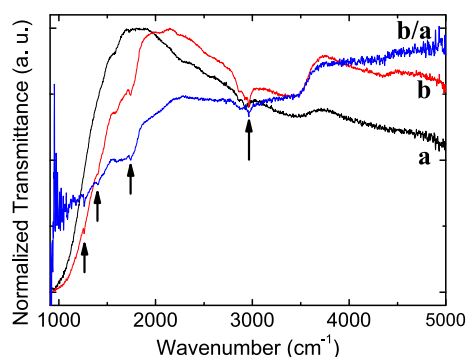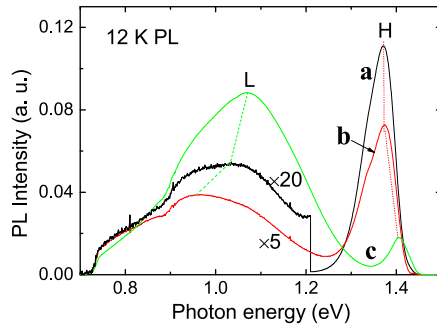

Fig. 2 FTIR transmittance spectra for the as-grown (**a**) and FE-treated (**b**) porous InP samples. The *arrows* indicate the positions of the absorption bands observed in the plotted frequency region

zones are voids and the bright zones are InP crystallites. The surface SEM images show uniform arrays of nearly square pores with an average pore diameter of approximately 120 nm and the wall thickness of around 40 nm. Figure 1c presents the chemical structure of the ferroelectric polymer, P(VDF–TrFE). It is a linear macromolecule with a large structural flexibility, and the change of the spontaneous polarization is caused by the rotation of the CF$_2$ functional groups [10].

Shown in Fig. 2 are the infrared transmittance spectra for the as-grown (a) and FE-treated (b) porous InP samples. Compared with the as-grown porous InP, there are several absorption bands in the FE-treated sample. The band near 1743 cm^{-1} is not predicted for this material, and is due to C=O stretching vibration caused by oxidation [11]. The 1262 cm^{-1}, 1402 cm^{-1}, and 2963 cm^{-1} bands can be attributed to the symmetric stretching vibration of CF$_2$ [12–17], the wagging vibration of CH$_2$ [16], and the symmetric stretching vibration of CH$_2$ [11], respectively. These ab-
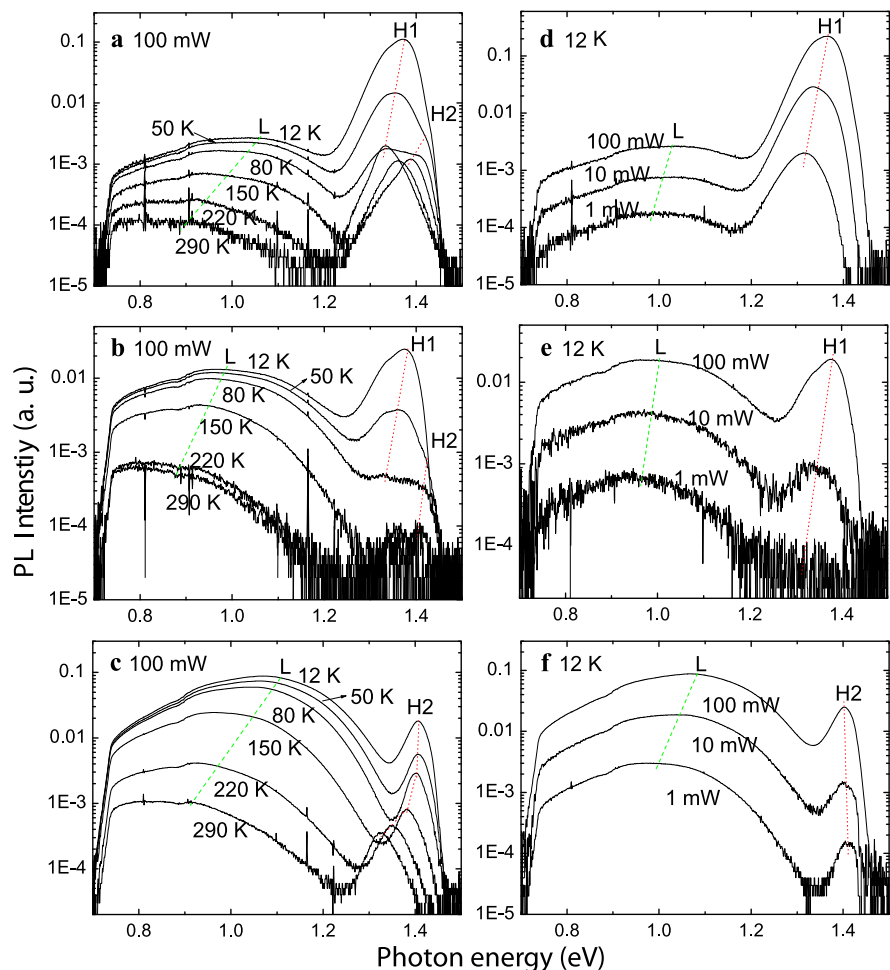
sorption bands are characteristics of the polymer P(VDF–TrFE), thus confirming the presence of the polymer in the FE-treated sample.

PL spectra at 12 K were investigated within the energy range of 0.7–1.5 eV, as shown in Fig. 3. It should be mentioned that no emission is observed in the present range for the ferroelectric polymers (not shown here). A broad emission band centered at about 1.0 eV (L band) appears in addi-

tion to the near-band-edge emission band at around 1.4 eV (H band), and the intensities and positions of the two emissions vary drastically in the three samples. In order to understand these phenomena, we obtained the PL spectra under various temperatures and excitation powers, as shown in Fig. 4. For clarity, the PL peak positions versus temperature and excitation power for the three samples are also presented in Fig. 5.
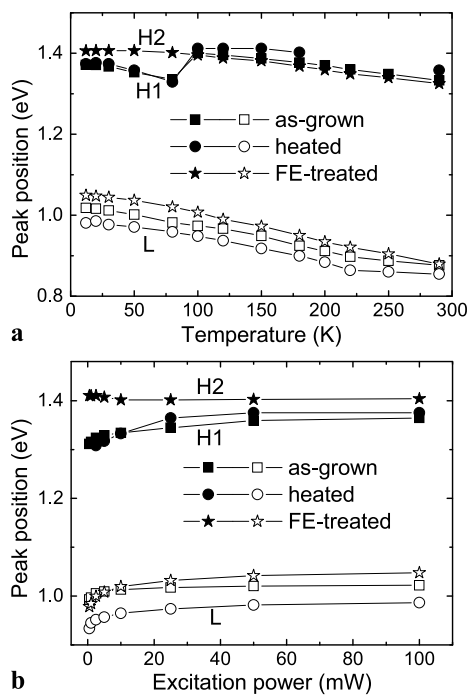
There are two components for the band 'H' of the as-grown and heated samples, and the peak position at each temperature agrees well with the reported value by Fujikura et al. [18]. The lower energy component 'H1' involves a continuum broad surface state at the pore wall surface, while the higher one 'H2' is assigned as the transition between electron and hole quantum states inside the pore wall. The temperature-dependent behaviors of emission 'H' in the as-grown and heated samples can be well explained by these assignments. It can also be clearly seen from Fig. 5a that the trend of the peak position of 'H' with temperature in the FE-treated sample is roughly parallel to 'H2' for the as-grown and heated samples, indicating that they have the same origin. On the other hand, the blue shift with increasing exci-

Fig. 3 PL spectra for the as-grown (**a**), heated (**b**), and FE-treated (**c**) porous InP samples measured at 12 K

Fig. 4 Temperature- and excitation-power-dependent PL spectra for the as-grown (**a**, **d**), heated (**b**, **e**), and FE-treated (**c**, **f**) porous InP samples

Fig. 5 The PL peak positions versus temperature (**a**) and excitation power (**b**) for the as-grown, heated, and FE-treated porous InP samples

tation power for emission 'H' in the as-grown and heated samples, as shown in Fig. 5b, is ascribed to the filling effect of surface energy levels [19]. However, a slight red shift is observed with increasing excitation power for the peak 'H' of the FE-treated sample, which is a general behavior in bulk InP due to the penetration effect of carriers [20]. It is consistent with the assignment of transitions between electron and hole states inside the pore wall from the temperature-dependent behaviors, implying that the surface states are passivated by ferroelectric polymers in the FE-treated sample. This surface passivation is confirmed by the following characteristics of a single component under various temperatures, a red shift with increasing excitation power and a blue shift with respect to the as-grown and heated samples. It is useful to passivate the surface states of porous InP by ferroelectric polymers for improving the performances of InP-based electronic and optoelectronic devices.

Due to the high dissociation phosphorus pressure, InP crystals have many intrinsic deep-level defects inducing radiative transitions. These emissions have been observed by PL between 0.9 and 1.2 eV, which is corresponding to the growth or annealing conditions. The emissions at 0.99, 1.21, and 1.08 eV at 77 K have been attributed to the donor-like phosphorus vacancy (V_P), the acceptor-like indium vacancy (V_{In}) or phosphorus interstitial (P_i), and a complex involving the two species of ($V_P V_{In}$) or ($V_P P_i$), respectively [21]. Thus, the band 'L' in the present work is associated with V_P. It can be clearly seen from Fig. 3 that the broad band 'L' is very weak in the as-grown sample, which increases

slightly after heat treatment and drastically after being FE treated. The out-diffusion of P is responsible for the intensity enhancement of band 'L' when using no protection during heat treatment [22]. Based on these results, we suggest that a possible ion exchange of P by F in the ferroelectric polymers induces a rather high concentration of V_P [23]; thus, the intensity of band 'L' enhances greatly in the FE-treated sample. It should also be noted that the band 'L' shows an opposite peak shift in the heated and FE-treated samples, which is caused by a change of deep-level centers or a variation in the coupling constant [24, 25]. In addition, the peak positions of band 'L' in the three samples have a similar dependence on temperature and excitation power, as shown in Fig. 5. The blue shift with increasing excitation power can be ascribed to the band-filling effect, while the red shift with increasing temperature is due to the Varshni effect [26].

4 Conclusion

In conclusion, the nanocomposites of porous InP infilled with ferroelectric polymers were investigated by temperature and excitation-power-dependent PL. A near-band-edge (NBE) emission centered at about 1.4 eV and a deep-level emission at around 1.0 eV due to phosphorus vacancies are observed for all the samples. The intensity suppression and blue shift of the NBE emission result from the passivation of surface states by introducing ferroelectric polymers. On the other hand, the significant enhancement of deep-level emission is caused by the increased concentration of phosphorus vacancies due to ion exchange when infilling the ferroelectric polymers into porous InP. The surface passivation of porous InP by ferroelectric polymers is useful for improving the performances of InP-based electronic and optoelectronic devices.

References

1. J. Lloyd-Hughes, S. Mueller, G. Scalari, H. Bishop, A. Crossley, M. Enachi, L. Sirbu, I.M. Tiginyanu, Appl. Phys. Lett. **100**, 132106 (2012)
2. T. Zhou, D.D. Cheng, M.J. Zheng, L. Ma, W.Z. Shen, Nanoscale Res. Lett. **6**, 276 (2011)
3. K. Busch, S. John, Phys. Rev. Lett. **83**, 967 (1999)
4. R. Heijden, C.F. Carlstrom, J.A.P. Snijders, R.W. Heijden, F. Karouta, R. Notzel, H.W.M. Salemink, R.K.C. Kjellander, C.W.M. Bastiaansen, D.J. Broer, E. Drift, Appl. Phys. Lett. **88**, 161112 (2006)
5. T.B. Xu, Z.Y. Cheng, Q.M. Zhang, R.H. Baughman, C. Cui, A.A. Zakhidov, J. Su, J. Appl. Phys. **88**, 405 (2000)
6. Q.M. Zhang, V. Bharti, X. Zhao, Science **280**, 2101 (1998)

7. M. Pientka, V. Dyakonov, D. Meissner, A. Rogach, D. Talapin, H. Weller, L. Lutsen, D. Vanderzande, Nanotechnology **15**, 163 (2004)

8. R. Korlacki, R.F. Saraf, S. Ducharme, Appl. Phys. Lett. **99**, 153112 (2011)

9. X.L. Che, L. Li, F.Q. Liu, X.Q. Huang, Z.G. Wang, Appl. Phys. Lett. **88**, 263107 (2006)

10. K. Asadi, D.M. Deleeuw, B.D. Boer, P.W.M. Blom, Nat. Mater. **7**, 547 (2008)

11. C. Welter, L.O. Faria, R.L. Moreira, Phys. Rev. B **67**, 144103 (2003)

12. S.T. Chen, K. Yao, F.E.H. Tay, C.L. Liow, J. Appl. Phys. **102**, 104108 (2007)

13. H.S. Xu, Z.Y. Cheng, D.N. Olson, T. Mai, Q.M. Zhang, Appl. Phys. Lett. **78**, 2360 (2001)

14. F. Xia, Z.Y. Cheng, H.S.H.F. Li, Q.M. Zhang, G.J. Kawaronos, R.Y. Ting, G.A. Sadek, K.D. Belfield, Adv. Mater. **14**, 1574 (2002)

15. H.S. Xu, D. Shen, Q.M. Zhang, Polymer **48**, 2124 (2007)

16. Z.J. Hu, M.W. Tian, B. Nysten, A.M. Jonas, Nat. Mater. **8**, 62 (2009)

17. C.W. Choi, A.A. Prabu, Y.M. Kim, S. Yoon, K.J. Kim, C. Park, Appl. Phys. Lett. **93**, 182902 (2008)

18. H. Fujikura, A.M. Liu, A. Hamamatsu, T. Sato, H. Hasegawa, Jpn. J. Appl. Phys. **39**, 4616 (2000)

19. A.M. Liu, C.K. Duan, Appl. Phys. Lett. **78**, 43 (2001)

20. S.D. Lester, T.S. Kim, B.G. Streetman, Appl. Phys. Lett. **52**, 474 (1988)

21. H. Temkin, B.V. Dutt, W.A. Bonner, Appl. Phys. Lett. **38**, 431 (1981)

22. J.K. Luo, T. Kimura, S. Yugo, Y. Adachi, Jpn. J. Appl. Phys. **26**, 582 (1987)

23. N. Kinrot, Y. Shapira, M.A.B. Moraes, Appl. Phys. Lett. **70**, 3011 (1997)

24. P.W. Yu, Solid State Commun. **34**, 183 (1980)

25. N. Duhamel, E.V.K. Rao, J. Cryst. Growth **64**, 186 (1983)

26. Y.P. Varshni, Physica **34**, 149 (1967)